



HAL
open science

Diverging temperature responses of CO₂ assimilation and plant development explain the overall effect of temperature on biomass accumulation in wheat leaves and grains

Iman Lohraseb, Nicholas C. Collins, Boris Parent

► **To cite this version:**

Iman Lohraseb, Nicholas C. Collins, Boris Parent. Diverging temperature responses of CO₂ assimilation and plant development explain the overall effect of temperature on biomass accumulation in wheat leaves and grains. *AoB Plants*, 2017, 10.1093/aobpla/plw092 . hal-01602749

HAL Id: hal-01602749

<https://hal.science/hal-01602749v1>

Submitted on 25 May 2020

HAL is a multi-disciplinary open access archive for the deposit and dissemination of scientific research documents, whether they are published or not. The documents may come from teaching and research institutions in France or abroad, or from public or private research centers.

L'archive ouverte pluridisciplinaire **HAL**, est destinée au dépôt et à la diffusion de documents scientifiques de niveau recherche, publiés ou non, émanant des établissements d'enseignement et de recherche français ou étrangers, des laboratoires publics ou privés.

OPEN ACCESS – RESEARCH ARTICLE

Diverging temperature responses of CO₂ assimilation and plant development explain the overall effect of temperature on biomass accumulation in wheat leaves and grains

Iman Lohraseb¹, Nicholas C. Collins¹, Boris Parent^{1,2}

¹ Australian Centre for Plant Functional Genomics, University of Adelaide, School of Agriculture Food and Wine, Hartley Grove, Urrbrae, South Australia 5064, Australia

² Current address: INRA, UMR759 Laboratoire d'Ecophysiologie des Plantes sous Stress Environnementaux. Place Viala, F-34060 Montpellier, France

boris.parent@supagro.inra.fr; iman.lohraseb@acpfg.com.au;

nick.collins@acpfg.com.au

Corresponding author: Boris Parent

boris.parent@supagro.inra.fr

Tel: +33 (0)4 99 61 31 83

Fax: +33 (0)4 67 52 21 16

Running title: Temperature response of biomass accumulation

Published by Oxford University Press on behalf of the Annals of Botany Company.

This is an Open Access article distributed under the terms of the Creative Commons Attribution License (<http://creativecommons.org/licenses/by/4.0/>), which permits unrestricted reuse, distribution, and reproduction in any medium, provided the original work is properly cited.

ABSTRACT

There is a growing consensus in the literature that rising temperatures influence the rate of biomass accumulation by shortening the development of plant organs and the whole plant and by altering rates of respiration and photosynthesis. A model describing the net effects of these processes on biomass would be useful, but would need to reconcile reported differences in the effects of night and day temperature on plant productivity. In this study, the working hypothesis was that the temperature responses of CO₂ assimilation and plant development rates were divergent, and that their net effects could explain observed differences in biomass accumulation. In wheat (*Triticum aestivum*) plants, we followed the temperature responses of photosynthesis, respiration and leaf elongation, and confirmed that their responses diverged. We measured the amount of carbon assimilated per “unit of plant development” in each scenario and compared it to the biomass that accumulated in growing leaves and grains. Our results suggested that, up to a temperature optimum, the rate of any developmental process increased with temperature more rapidly than that of CO₂ assimilation and that this discrepancy, summarised by the CO₂ assimilation rate per unit of plant development, could explain the observed reductions in biomass accumulation in plant organs under high temperatures. The model described the effects of night and day temperature equally well, and offers a simple framework for describing the effects of temperature on plant growth.

Keywords: Biomass; development; grain growth; photosynthesis; respiration; specific leaf area; temperature; thermal time; wheat.

INTRODUCTION

High temperatures decrease biomass accumulation in plant leaves (Vile *et al.* 2012), cereal grains (Wheeler *et al.* 1996) and whole plants, with implications for agricultural productivity and ecology under a climate change scenario (Peng *et al.* 2004). An emerging consensus is that carbon balance is a critical factor in responses of biomass accumulation processes to temperature changes. This view comes from studying temperature responses of grain dry mass (Wardlaw 1994; Wheeler *et al.* 1996), and leaf dry mass per area (LMA) or its reciprocal, the specific leaf area (Poorter *et al.* 2009). Most of these studies investigated the effect of very high temperatures within the “stressing range” where photosynthesis was demonstrated to be negatively affected (Lovey *et al.* 2002; Vasseur, Pantin & Vile 2011). Accordingly, high CO₂ or light, which increases photosynthesis, can partially offset the impact of high temperature on biomass accumulation in vegetative tissues (Taub, Seemann & Coleman 2000; Vasseur *et al.* 2011) and in grains (Wardlaw 1994; Wheeler *et al.* 1996).

By contrast, rising temperatures in the “non-stressing” temperature range increase the rate of photosynthesis (Atkin & Tjoelker 2003; Sage & Kubien 2007). One consequence is accelerated dry weight accumulation in the grain (Wheeler *et al.* 1996), which reflects faster accumulation of photosynthate. High temperatures also accelerate cell expansion and division, and hasten genetic programs of organ differentiation, consequently shortening the period over which biomass can accumulate (Parent *et al.* 2010b). These effects are largely independent of variations in carbon fixation (Morita *et al.*, 2005).

Temperature during grain filling impacts final single grain weight with effects on both the rate and duration of grain filling (Sofield *et al.* 1977; Yin, Guo & Spiertz 2009). Similarly, temperature influences LMA by impacting photosynthesis and the rates of leaf expansion (Tardieu, Granier & Muller 1999).

Predicting temperature effects on biomass accumulation requires an understanding of the dynamics of carbon assimilation and plant development responses. The temperature response of respiration and photosynthesis are now well-described under the “non-stressing” temperature range (Atkin *et al.* 2003; Sage *et al.* 2007). These responses are divergent (Atkin, Scheurwater & Pons 2007), and both change after exposure to a period of high temperature, *i.e.*, they show acclimation behaviour (Atkin, Scheurwater & Pons 2006; Campbell *et al.* 2007). Parent & Tardieu (2012) demonstrated that multiple developmental processes followed a common temperature response curve within a given species. Indeed, rates of processes as diverse as leaf expansion, progression towards flowering or other developmental milestones (*e.g.*, percentage of final grain fill duration per day = grain development rate), shared similar temperature responses and are hereafter referred to as ‘development rates’. The temperature responses of these developmental processes followed different patterns to photosynthesis, and other enzymatic reactions involved in primary metabolism (Parent *et al.* 2010a).

However, in crop temperature response models, different formalisms are currently used to describe development and leaf expansion (Parent *et al.*,

2014; Kumudini et al., 2014). Predicted responses of development to temperature depend on the chosen equation and its parameterisation, and few models consider equations that accommodate different day and night temperature (example: Crop Heat Unit, reviewed by Kumudini et al., 2014), or different plant stages. There are currently efforts from the community of crop modellers to make these equations converge (Makowsky *et al.*, 2015) with suites of tools such as APSIM (Rosenzweig *et al.*, 2013). The same applies to the response of photosynthesis or radiation use efficiency, with several equations used in the various models (reviewed in Parent et al., 2014). While many crop models consider specific leaf area to be a result of leaf expansion and biomass, many others consider SLA as a genetic parameter with leaf expansion being driven by leaf biomass (reviewed in Parent et al., 2014). In addition, there is still debate about specific night temperature effects on biomass or production (Peraudeau et al., 2015; Fang et al., 2015; Glaubitz et al., 2014; Kanno et al., 2010; Peng et al., 2004).

Due to the different and non-linear temperature response curves of development rate, photosynthesis, and respiration, the relative impacts of these component traits on biomass accumulation (and their temperature dynamics) would depend on the particular growth temperature range. Here, we address these divergences by using rates of respiration, photosynthesis and various developmental processes observed across a range of thermal scenarios in wheat to model the temperature responses of these traits. We then express net photoassimilate accumulation per “unit of leaf development” or “unit of grain development” or “unit of whole plant development” at a given temperature in terms of the equivalent value at 20°C. As such, this approach

provides a framework for describing the relative contributions of photosynthesis and respiration to biomass accumulation across a temperature range, with reference to a standard unit.

METHODS

Plant growth conditions

All experiments were carried out with the bread wheat (*Triticum aestivum*) cultivar Apogee. Seeds were sown in plastic pots (8 x 8 x 20 cm) filled with a coir-peat-based potting mix. Plants were grown in several identical growth chambers (GC-20 Bigfoot series, BioChambers, Winnipeg, Canada). Light was supplied by fluorescent bulbs (Photosynthetically Active Radiation, PAR = $380 \mu\text{mol m}^{-2} \text{s}^{-1}$) for 12 h of photoperiod (PP) with an overall daily PAR ($3.6 \pm 0.1 \text{ MJ m}^{-2} \text{ d}^{-1}$) similar to that observed in the field at vegetative stage (O'Connell *et al.*, 2004). CO₂ naturally varied during the day but daily average CO₂ concentration was similar in all treatments. In each of the three experiments, plants were initially grown under temperatures of 25°C day (T°_{day}) and 20°C night (T°_{night}) and the soil was watered close to the saturation level.

In Experiment 1, plants were transferred to different constant temperatures (11, 17, 20, 23 and 29°C) at appearance of leaf 6. Leaf temperature, measured with an infrared thermometer (Raynger MX4, Raytek Corporation, Santa Cruz, CA, USA), was close ($\Delta T^{\circ} < 1^{\circ}\text{C}$) to the air temperature, during both nights and days. Because air relative humidity was stable in all treatments ($60 \pm 5\%$), vapor pressure deficit varied from 0.5 kPa at 11°C to 1.8 kPa at 29°C.

In Experiment 2, plants at the appearance of leaf 4 were transferred to several thermal regimes ($T^{\circ}_{\text{day}}/T^{\circ}_{\text{night}}$: 20/15, 20/20, 25/15 and 25/20 °C)

where they remained until anthesis (appearance of first anthers on the main spike).

In Experiment 3, plants at anthesis were transferred to several thermal regimes ($T^{\circ}_{\text{day}}/ T^{\circ}_{\text{night}}$: 20/15, 20/20, 25/15 and 25/20 °C) where they remained until maturity. At heading (head of the main tiller fully emerged), plants were pruned leaving the main tiller with its 3 youngest leaves. New tillers were then removed weekly.

Leaf measurements

In Experiments 1 and 2, leaf elongation rate (LER) was measured on leaf 6, by measuring leaf length with a ruler, at leaf appearance and again after a further 24 h. In parallel, it was determined that this developmental stage corresponded to the linear phase of elongation under all tested thermal scenarios (data not shown).

In Experiments 1 and 2, photosynthesis rate during the day and respiration rate during the night were analyzed on fully-developed leaf 4 when leaf 6 was elongating, using a gas exchange system (LI-6400, Li-Cor, Lincoln, NE). Photosynthesis was measured at least 2 hours after lights were switched on and 2 hours before lights were switched off. Artificial illumination was supplied from a red-blue LED light source with $\text{PAR} = 380 \mu\text{mol m}^{-2} \text{s}^{-1}$, similar to the growth chambers, or under saturating light ($\text{PAR}=2000 \mu\text{mol m}^{-2} \text{s}^{-1}$). Respiration rate during the night was measured at predawn, during the last 3 hours of the night cycle. CO_2 was maintained at 400 ppm (Reference) using the CO_2 mixer (flow rate = $500 \mu\text{mol s}^{-1}$).

Daily net photosynthesis rate during the day (P_N , mol m⁻² d⁻¹) and daily respiration rate during the night (R , mol m⁻² d⁻¹) were calculated by integrating the measured instantaneous rates of photosynthesis and respiration during the night during the respective times of light and dark (12 h) to arrive at a daily integral. The overall net CO₂ assimilation rate per day (A_N , mol m⁻² d⁻¹) was calculated:

$$A_N = P_N - R \quad (\text{Eq.1})$$

Unless indicated otherwise, values of A_N and P_N used were those measured at PAR = 380 μmol m⁻² s⁻¹.

In Experiment 2, leaves 4, 5, 6 and 7 were collected at anthesis. Leaf length was measured with a ruler, leaf area was measured with a planimeter (PATON electronic belt driven planimeter, CSIRO, Canberra, Australia) and leaf dry weight was determined after 2 days at 85°C.

Data analysis

The R language (R Development Core Team, 2005) was used for all statistical analyses and model regressions, namely comparison of means (function *pairwise.t.test* with “BH” method), Pearson correlation tests (function *cor.test*), linear regression (function *lm*), non-linear regression (function *nls*) and analysis of variance (function *anova*). Data and scripts are available on demand.

Temperature responses

Temperature responses were described by the equation of Johnson, Eyring and Williams (1942), modified by Parent *et al.* (2012):

$$F(T) = \frac{ATe^{\left(\frac{-\Delta H_A^\ddagger}{RT}\right)}}{1 + \left[e^{\left(\frac{-\Delta H_A^\ddagger}{RT}\right)} \right]^\alpha \left(1 - \frac{T}{T_0}\right)} \quad (\text{Eq.2})$$

where $F(T)$ is the considered rate, T is the temperature (Kelvin, K), ΔH_A^\ddagger (J mol⁻¹) is the enthalpy of activation of the process and determines the curvature at low temperature, α (dimensionless) determines how sharp is the decrease in rate at high temperature and is fixed at 3.5 for development processes (Parent *et al.* 2012), T_0 (K) determines the temperature at which the rate is maximum, and A is the trait scaling coefficient. Temperature responses of LER, P_N , and R were calculated by non-linear regressions on values measured in Experiment 1. The response of A_N to temperature was then calculated from the temperature responses of R and P_N , using Eq.1.

Thermal compensation of time and rates

For any measured rate $J(T)$ at temperature T , a temperature compensated rate was calculated as the equivalent rate at 20°C.

$$J_{20^\circ\text{C}} = J(T) \frac{F(20^\circ\text{C})}{F(T)} \quad (\text{Eq.3})$$

with $F(T)$ being the response of development to temperature (here the response of LER). Because developmental time (or thermal time $t_{20^{\circ}\text{C}}$) is the reciprocal of development rate, it results in:

$$t_{20^{\circ}\text{C}} = t(T) \frac{F(T)}{F(20^{\circ}\text{C})} \quad (\text{Eq.4})$$

Such a procedure was already applied in different studies of developmental processes (Louarn, Andrieu & Giauffret 2010; Parent, Conejero & Tardieu 2009; Parent *et al.* 2010b), and was applied here for biomass accumulation processes and net CO_2 assimilation rate (A_N).

In Experiment 2 and 3, $\frac{F(20^{\circ}\text{C})}{F(T)}$ was calculated in each thermal treatment from LER values directly measured in Experiment 2. In the other cases, $\frac{F(20^{\circ}\text{C})}{F(T)}$ was inferred from the regression function $LER(T)$.

Leaf senescence profiles

In Experiment 3, chlorophyll content was measured with a SPAD chlorophyll meter (Minolta, Plainfield, Illinois, USA). Each measurement was the average of 15 readings: 5 taken from along each of the three last-developed leaves. In each treatment, four plants were measured repeatedly: at anthesis and at 7, 13, 19, 25, 31, 38, 42 and 46 days after anthesis.

In each thermal scenario, a bilinear model was fitted to the dataset (see SUPPORTING INFORMATION Methods S1). It comprised a constant value (SPAD_0) until a time of senescence (t_s), followed by a linear decrease in content after this point, with a slope a_s . Because plants had the same thermal treatment before anthesis, SPAD_0 was fixed for all thermal scenarios and

equalled the average value at anthesis for all treatments ($SPAD_0=57.3$). A similar procedure was carried out considering time t and t_s as developmental time ($t_{20^\circ C}$ and $t_{s,20^\circ C}$, $d_{20^\circ C}$).

Biomass accumulation in the grain

In Experiment 3, the main spikes of four plants per thermal scenario were collected at 7, 13, 19, 25, 31 days after anthesis and at grain maturity, and seed number and average single grain dry weight (GDW) were measured after three days at $85^\circ C$. Spikes with fewer than 30 seeds were not used in the analysis (6 in total were discarded from the whole experiment; $n \geq 3$ was used for all sampling dates and thermal treatments).

Curves of biomass accumulation in the grain can be described with a 3 parameter logistic equation (Morita *et al.* 2005), modified here to obtain the theoretical grain weight at anthesis (W_0 , mg) as a parameter of the following equation (see SUPPORTING INFORMATION Methods S1):

$$W(t) = \frac{W_0(1+e^{\lambda t_0})}{1+e^{(-\lambda(t-t_0))}} \quad (\text{Eq.5})$$

$W(t)$ is the weight of one seed (mg) at time t (in days) after anthesis, λ (in d^{-1}) is the slope factor controlling the steepness of the curve and t_0 is the inflection point, or time at which the seed is half the final weight. Because plants were transferred to the different thermal treatments at anthesis, W_0 was considered as common in all treatments ($W_0=1.65$ mg, see SUPPORTING INFORMATION Methods S1).

Eq.5 was fitted in each thermal scenario, considering either time or developmental time ($t_{20^{\circ}\text{C}}$ in $d_{20^{\circ}\text{C}}$). In the last case, the two free parameters are expressed with developmental time units ($t_{0,20^{\circ}\text{C}}$ in $d_{20^{\circ}\text{C}}$; $\lambda_{20^{\circ}\text{C}}$ in $d_{20^{\circ}\text{C}}^{-1}$). Because $t_{0,20^{\circ}\text{C}}$ values were similar between treatments, a single $t_{0,20^{\circ}\text{C}}$ value common to all treatments was determined (see SUPPORTING INFORMATION Methods S1). Respective values of t_0 were then calculated in each treatment. In this case, λ is the only free parameter.

The grain growth rate $GGR(t)$, was obtained by derivation of Eq.5 (see SUPPORTING INFORMATION Methods S1). Grain growth rate is maximal (GGR_{max}) at the inflection point, namely t_0 .

$$GGR_{\text{max}} = GGR(t_0) = \frac{\lambda W_0(1+e^{\lambda t_0})}{4} \quad (\text{Eq.6})$$

with time and model parameters expressed either with time or developmental time units.

Note that with $t_{0,20^{\circ}\text{C}}$ and W_0 fixed, $GGR_{\text{max},20^{\circ}\text{C}}$ depends only on $\lambda_{20^{\circ}\text{C}}$ (and the reciprocal, $\lambda_{20^{\circ}\text{C}}$ depends only on $GGR_{\text{max},20^{\circ}\text{C}}$). $GGR_{\text{max},20^{\circ}\text{C}}$ alone can therefore explain the kinetics of grain growth rate.

Grain filling duration (t_f) was calculated as the duration between anthesis and the time at which the grain reached 95% of its final weight (see SUPPORTING INFORMATION Methods S1).

$$t_f = -\frac{1}{\lambda} \ln \left[\frac{5}{95} \right] + t_0 \quad (\text{Eq.7})$$

Grain growth simulations

For any thermal scenario, a time series (0 to 100 days after anthesis, time step =1 d) was built, with corresponding photoperiod $PP(t)$, $T^{\circ}_{day}(t)$, $T^{\circ}_{night}(t)$ and $T^{\circ}_{ave}(t)$. $t_{20^{\circ}C}(t)$, $P_N(t)$, $R(t)$ were calculated from parameters of Eq.2 (parameter values differing between processes). $A_{N,20^{\circ}C}(t)$ was calculated from Eq.1 and 3. $\lambda_{20^{\circ}C}(t)$ was inferred from the linear relationship between $\lambda_{20^{\circ}C}$ and $A_{N,20^{\circ}C}$ obtained in Experiment 3. $GGR_{20^{\circ}C}(t)$ was calculated (see SUPPORTING INFORMATION Methods S1) and individual grain weight was then obtained at each t by numerically integrating $GGR_{20^{\circ}C}$ between anthesis and the corresponding $t_{20^{\circ}C}(t)$.

$$W(t) = W(t_{20^{\circ}C}) = W_0 \int_{x=0}^{t_{20^{\circ}C}} GGR_{20^{\circ}C}(x) dx$$

(Eq.8)

Data from the literature

Some data were collected from the literature (Alkhatib & Paulsen 1984; Tashiro & Wardlaw 1990; Wardlaw *et al.* 2002; Wardlaw, Dawson & Munibi 1989a; Wardlaw *et al.* 1989b; Zahedi, Sharlma & Jenner 2003; Zhao *et al.* 2007) and are summarized in SUPPORTING INFORMATION Table S1. The positions of data points were recorded in figures by image analysis (software ImageJ; <http://rsbweb.nih.gov/ij/>). The grain weight reductions between thermal treatments found in these studies were compared to simulations carried out with the above procedure.

RESULTS

Net CO₂ assimilation rate per unit of plant development decreased when temperature rose.

In plants where leaf 6 was emerging, rate of leaf 6 elongation (LER) was measured at five constant temperatures in the range 11 to 29 °C (Fig.1a; Experiment 1, n > 8). The equation of Johnson *et al.* (1942) modified by Parent *et al.* (2012) fitted well with experimental data (Fig.1a, R²=0.99) with response parameters ($\square H_A^\ddagger=69.1 \text{ kJ mol}^{-1}$; $T_0 = 29.2^\circ\text{C}$) close to those previously determined in the meta-analysis of Parent *et al.* (2012). The temperature response curves of net day photosynthesis (P_N) and dark respiration (R) were also both adequately described by this equation (Fig.1b, n > 4, R² = 0.99 and 0.97, respectively). Response of respiration was not far from that of development ($\square H_A^\ddagger=74.9 \text{ kJ mol}^{-1}$) but the slope of P_N was flatter under rising temperatures, as indicated by the low value of $\square H_A^\ddagger$ (19.3 kJ mol⁻¹). When measured under saturating light, the response of photosynthesis was steeper ($\square H_A^\ddagger=36.2 \text{ kJ mol}^{-1}$, not shown) but still less than that of respiration or development. The temperature response curve of the net CO₂ assimilation per day (A_N, Fig.1b) was then calculated from P_N and R (Eq.1).

Temperature response curves were normalized so that they intersected the same value at 20°C (Fig.1c), facilitating the comparison in the absence of any differences in units or magnitude (Parent *et al.* 2010a). Because leaf elongation is part of the multitude of development processes sharing a common response to temperature (Parent *et al.* 2010 & 2012), this temperature response of normalized LER was considered as the response of

development processes to temperature. It was used to adjust times and rates of other processes by the effect of temperature on general development (developmental time calculation).

Development rate accelerated more than carbon assimilation rate as temperature increased, until the optimum temperature was reached (26.6 and 25.5 °C for LER and A_N , respectively). Under saturating light, the two responses were more similar, although development still accelerated more than A_N (data not shown). Expressing A_N per unit of developmental time ($A_{N,20^\circ\text{C}}$) can be thought as an amount of carbon assimilated per standard unit of leaf elongation (and by inference, per unit of any developmental process). $A_{N,20^\circ\text{C}}$ decreased when temperature rose across the measured range (Fig.1d), indicating that the amount of assimilated carbon available per unit of development decreased under rising temperatures.

Net CO₂ assimilation rate per unit of leaf development was linked to the dry mass per leaf area for plants grown under different thermal regimes without an additional effect of night temperature.

Various scenarios of day/night temperature were applied at appearance of leaf 6 to allow net CO₂ assimilation rate to be viewed independently of development (Fig.2; Experiment 2, n = 6). LER increased about equally under increasing T°_{night} or T°_{day} (Fig.2a), and was therefore essentially the same under thermal scenarios ($T^\circ_{\text{day}}/T^\circ_{\text{night}}$) 20/20°C and 25/15°C. By contrast, R only increased under rising T°_{night} and P_N only increased under rising T°_{day} (see SUPPORTING INFORMATION Table S2). Because P_N

values were much higher than R values and explained most of the variance in A_N (not shown), significant differences in A_N were only observed when T_{day} differed (Fig. 2b). Therefore, treatment comparisons where only the night temperature differed (20/15 vs. 20/20 °C, or 25/15 vs. 25/20 °C) showed differences in LER with essentially no change in A_N . Conversely, the comparison 25/15 vs. 20/20 °C showed differences in A_N with essentially no change in LER. Overall, these thermal treatments resulted in contrasting CO_2 assimilation rates per unit of developmental time (Fig.2c), viewed here as the amount of assimilated carbon available per unit of leaf development.

The leaf dry mass per area (LMA), measured at anthesis on leaves 4, 5, 6 and 7, was affected by thermal treatments in all leaves (see SUPPORTING INFORMATION Figure S1), even in leaves 4 and 5, which were already partly elongated before applying the different thermal scenarios.

Consequently, the average LMA in the 4 measured leaves differed significantly between treatments (Fig. 2d). These differences were mostly due to differences in leaf biomass rather than leaf area (respectively explaining 86.2% and 2.7% of the total variance, not shown). A temperature-induced rise in A_N while maintaining similar leaf expansion rate would increase the amount of assimilated carbon per unit of leaf area expansion. Accordingly, LMA was significantly greater in the 25/15°C treatment than in the 20/20°C treatment ($60.0 \pm 4.1\text{g}$ versus $41.4 \pm 3.8 \text{ g m}^{-2}$, Fig.2d).

Conversely, a temperature-induced increase in LER without any changes in A_N would decrease the amount of assimilated carbon per unit of leaf expansion. Accordingly, LMA was less under 20/20°C than 20/15°C (41.4 ± 3.8 versus $51.6 \pm 2.5 \text{ g m}^{-2}$), and less under 25/20°C than 25/15°C ($45.4 \pm$

2.9 versus $60.0 \pm 4.1 \text{ g m}^{-2}$). Overall, $A_{N,20^\circ\text{C}}$ showed a strong positive correlation with LMA (Fig.2e, $R^2 = 0.96$; $p = 0.022$ in a Pearson correlation test). Therefore, $A_{N,20^\circ\text{C}}$ integrated the temperature effects on leaf expansion rate and CO_2 assimilation rate to explain differences in LMA observed between these different thermal scenarios.

Rates of progress towards grain maturity and leaf senescence depended only on temperature response of development

Plants at anthesis were introduced to several temperature scenarios, and then leaf senescence and biomass accumulation in the grain were measured over time (Fig.3a and Fig.4a; Experiment 3; $n > 4$ for each time point).

Chlorophyll content in the three last developed leaves, defined in SPAD units, was at first stable, and then decreased linearly. Fitting a bilinear model enabled the calculation of the time at which the chlorophyll level started to decrease (t_s). This parameter was closely correlated with the average daily temperatures (from 20.0 ± 1.7 at $25/20^\circ\text{C}$ to 26.5 ± 3.4 d at $20/15^\circ\text{C}$, Fig.3a.inset). When time and model parameters were expressed in developmental time units (Fig.3b), profiles of leaf senescence were similar between thermal treatments ($t_{s,20^\circ\text{C}}$ ranging from 21.8 ± 3.4 to 23.2 ± 3.7 $\text{d}_{20^\circ\text{C}}$; Fig.3b.inset).

Fitting logistic curves (Eq.5) to the time courses of single grain dry weight (GDW; Fig.4a) resulted in various values of t_0 , the time at which grain weight reached half of the final dry weight and growth was maximal (Fig.4a.inset). Its values decreased with rising average temperatures (from 24.0 ± 0.5 to $17.9 \pm$

0.7 d). Similarly, the time taken for complete grain fill (t_f) decreased by 11 d with rising temperatures (from 46.6 to 35.1 d, not shown). However, grain filling duration was similar in the 25/15 and 20/20 °C treatments (36.8 d and 38.4 d, not shown) indicating that it was largely independent of carbon assimilation. When time was expressed in developmental time units ($d_{20^\circ\text{C}}$, Fig.4b), values of $t_{0_20^\circ\text{C}}$ were similar across treatments (ranging from 19.8 ± 0.3 to 21.6 ± 0.7 $d_{20^\circ\text{C}}$, Fig.4b.inset) as were values of grain filling duration (from 39.2 to 42.3 $d_{20^\circ\text{C}}$, not shown).

Overall, rates toward grain maturity and rates of leaf senescence were similar across thermal treatments when expressed in developmental time. Grain filling duration was only dependent on average temperature, and mostly independent of carbon supply.

Maximum rates of biomass accumulation in individual grains were dependent on net CO₂ assimilation but independent of development rates.

Time courses of biomass accumulation in the grain were adequately described by the logistic model when only one parameter (λ) was kept free in each thermal scenario (W_0 and $t_{0_20^\circ\text{C}}$ fixed in all treatments, Fig.4c, $t_{0_20^\circ\text{C}} = 20.2$ $d_{20^\circ\text{C}}$; see Material and Methods and see SUPPORTING INFORMATION Methods S1).

As the maximum rate of accumulation of dry weight in single grains (GGR_{max}) and λ are interdependent variables (Eq.6), grain growth responses to temperature are hereafter described in terms of GGR_{max} only (more intuitive than λ). GGR_{max} varied between thermal treatments, especially where day

temperature differed (Fig.4c and 5a). Because temperature accelerated leaf senescence and progress towards grain maturity similarly, effects of temperature on rates of grain dry weight accumulation could not be attributed to one or the other of these factors.

Relative to the 25/15°C treatment, the 20/20°C treatment showed an increase in CO₂ assimilation (A_N) and GGR_{max} (1.18 ± 0.01 to 1.44 ± 0.02 mg d⁻¹, Fig.5a) but a similar rate of progress toward grain maturity. By contrast, increasing night temperature, i.e., 20/15 vs. 20/20 °C, or 25/15 vs. 25/20 °C, increased development rate but not A_N or GGR_{max} (Fig.5a). Therefore, GGR_{max} appeared to be only dependent on carbon assimilation rate and largely independent of development rate.

Overall, the two contributors to final grain weight, the rate toward grain maturity and the rate of biomass accumulation in the grain, behaved independently, and correlated with temperature responses of development and of carbon assimilation, respectively.

Net CO₂ assimilation rate expressed in developmental units explained the differences in dynamics of grain biomass accumulation.

When expressed in developmental units, maximum grain growth rate (GGR_{max.20°C}, Fig.5a) was dependent on both the rate of development and of CO₂ assimilation. GGR_{max.20°C} can be thought as the biomass accumulation per standard unit of grain development. In the same way, A_N expressed per unit of developmental time ($A_{N.20°C}$) can be thought as the amount of assimilated carbon available per unit of grain development. An increase in

CO₂ assimilation for a similar grain development rate increased $GGR_{\max,20^{\circ}\text{C}}$ (20/20 vs. 25/15 °C; 1.18 to 1.40 mg d_{20°C}⁻¹, Fig.5a). Increasing the grain development rate without increasing the CO₂ assimilation rate resulted in lower $GGR_{\max,20^{\circ}\text{C}}$, as shown in treatments 20/15 vs. 20/20 °C or 25/15 vs. 25/20 °C, Fig.5a). $A_{N,20^{\circ}\text{C}}$ was positively correlated with $GGR_{\max,20^{\circ}\text{C}}$ (Fig.5b, $R^2 = 0.97$, $p = 0.009$ in a Pearson correlation test). Because $GGR_{\max,20^{\circ}\text{C}}$ could completely describe the time course of biomass accumulation, $A_{N,20^{\circ}\text{C}}$ was correlated with final grain weight (Fig.5b, $R^2 = 0.98$, $p = 0.005$ in a Pearson correlation test).

Overall, by integrating the temperature effects on the rates of grain development and CO₂ assimilation, $A_{N,20^{\circ}\text{C}}$ was able to explain the differences in grain growth rate and final grain weight observed between the different thermal scenarios.

This relationship was used to simulate final grain weight effects reported in seven different papers for various thermal scenarios involving T°_{day} up to 30°C and T°_{night} up to 25°C (Fig.6). The predicted grain weight reductions were not far from the observed ones ($R^2=0.79$), suggesting that the relationship between $A_{N,20^{\circ}\text{C}}$ and grain growth rate could hold true for other genotypes, environmental conditions, and thermal scenarios within the investigated range. However, the model had a tendency to over-estimate the negative effect of rising temperatures (average bias of 16%), indicating a genetic variability for this relationship, or the influence of other physiological processes such as carbon remobilization to the grains.

DISCUSSION

Temperature response patterns of biomass accumulation in leaves and grains as a consequence of the discrepancy between development and carbon assimilation responses.

Various studies have emphasized a role of altered carbon supply-demand in the effects of high temperature on plant processes (Taub *et al.* 2000; Vasseur *et al.* 2011; Vile *et al.* 2012). Yet, this concept has rarely been tested by concurrently monitoring temperature responses of development, carbon assimilation and biomass accumulation (Poorter *et al.* 2009), or in a range of temperatures that were not harmful to photosynthesis (Vasseur *et al.* 2011; Vile *et al.* 2012). Therefore, we simultaneously monitored the temperature responses of development, respiration and photosynthesis in the non-stressing range. These responses were divergent, resulting in a variation in carbon supply relative to development across various thermal treatments. Under rising temperatures, an increase in photosynthesis increased both LMA and grain weight, while accelerated development reduced leaf and grain weights. We showed that the discrepancy between the temperature responses of development and carbon assimilation could explain the observed patterns of biomass accumulation in wheat leaves and grains across a range of thermal scenarios.

Expressing net CO₂ assimilation and biomass accumulation per unit of development summarizes the effects of temperature on development and carbon assimilation.

Here, we examined the possibility of using the thermal compensation of time and rates to dissect factors influencing biomass accumulation. Previously, this concept was applied to enable the effects of other environmental variables on leaf expansion (Parent *et al.* 2010b), cell expansion profiles in leaf (Parent *et al.* 2009) or endogenous rhythms (Poire *et al.* 2010) to be studied independently of the effect of temperature on development. In the current study, by expressing the rates of processes not classified as “development processes”, such as biomass accumulation in tissues, in terms of rate per unit of development, we were able to quantify the component of biomass accumulation response that was controlled purely by fluctuations in net carbon assimilation. Expressing the net assimilation rate in terms of developmental time therefore summarized the effects of temperature on photosynthesis, respiration and development. It can be thought as the ratio of source / development sink, or as the amount of assimilated carbon available per unit of plant development. In addition, a simple model using this trait as the indicator of source-sink dynamics was able to explain most of the effects of thermal scenarios on grain weight, across different genotypes and environmental conditions.

By allowing the contribution of net carbon fixation on biomass accumulation across a temperature range to be followed independently of the effect of temperature on development, this approach makes possible an assessment of the impact of other factors (e.g. light intensity) on biomass accumulation

across a range of temperatures. Furthermore, it could provide an approach for quantifying longer lasting heat damage caused by factors such as protein denaturation that are likely encountered at much higher temperatures, independent of reversible responses of a purely thermodynamic nature.

Rising night temperature is likely to decrease biomass production

Increasing either night or day temperature would accelerate development by the same degree (Morita *et al.* 2005; Parent *et al.* 2010a), but only increases in T°_{night} would increase respiration without any compensatory increase in photosynthesis. Simple simulations also indicate that $A_{N,20^{\circ}\text{C}}$ would be more sensitive to an increase in T°_{night} than to a similar increase in T°_{day} or the 24-h average temperature T°_{ave} (not shown). Indeed, our own experiment employing four day/night thermal treatments demonstrated that increasing T°_{night} reduced grain biomass more than increasing T°_{day} or T°_{ave} . In the simulation shown in SUPPORTING INFORMATION Figure S2, increasing night temperature by 5°C decreased $A_{N,20^{\circ}\text{C}}$ from 1.33 to 1.09 mol m⁻² d_{20°C}⁻¹ (not shown) and therefore decreased final grain weight by 15.3%.

The effect of maximum daily temperature (T_{max}) and minimum daily temperature (T_{min} ; which occurs during the night) on the performance of wheat and rice in the field has been examined using data across multiple environments. Such studies have revealed greater and more frequent negative impacts of warming during the night than warming during the day (Peng *et al.* 2004; Welch *et al.* 2010; Lobell & Ortiz-Monasterio 2007; Cossani & Reynolds 2012). Our findings offer a potential explanation for

these differential effects of day and night temperature on crop productivity in the field. In this study, no additional “hidden” effect of night temperature was detected.

Could temperature acclimation change this pattern?

While temperature changes in the non-stressing range can perturb photosynthesis and respiration in the short-term, the rates of these two processes can eventually recover completely, due to acclimation (Atkin *et al.* 2006; Campbell *et al.* 2007). Acclimation might make net CO₂ assimilation insensitive to any long-term temperature change (Atkin *et al.* 2006). By contrast, development rate was found to be stably dependent on temperature, and did not acclimate (Parent *et al.* 2012). Therefore, it is possible that long term responses of biomass accumulation to rising temperature, such as those experienced across the seasons, may only depend on the temperature responses of development, resulting in a greater reduction in biomass (mass per unit of development) than is predicted from the presented model. The model may apply better to day to day fluctuations, such as brief heat waves of several days duration, which commonly occur in the southern Australian wheat belt during the flowering and grain filling period and correlate with significant grain yield losses (Wardlaw and Wrigley 1994; Telfer *et al.* 2013).

Diversity of biomass accumulation responses

The temperature response of CO₂ assimilation per unit of plant development can present a large diversity. Firstly, there is a large diversity between plant species for the temperature responses of photosynthesis and respiration rates (Loveys *et al.* 2002), as well as for temperature acclimation of these processes (Atkin *et al.* 2006). In addition, there is a large genetic variability for development rate *per se* (Borras-Gelonch *et al.* 2010). The temperature response of development, while highly conserved in each species presented also a large variability between species (Parent *et al.* 2012). It follows that the overall response of the net assimilation per unit of plant development could present a large diversity between genotypes or species.

Grain biomass and yield in a broad sense do not depend only on the total assimilated carbon. A large genetic variability can be found in the ability of plants to mobilize and allocate carbon to the grains (Reynolds *et al.* 2009). It probably explains why the model over-estimated the effects of temperature on grain size in Figure 6. These processes have their own response to temperature (Poorter *et al.* 2012) and can therefore present interesting genetic variability. In wheat, improving photosynthesis efficiency and partitioning to the grain are the central targets of the International Wheat Consortium (IWC, Reynolds *et al.* 2011).

The presented model was intentionally simple, used only to test the presented hypothesis, that the discrepancy between CO₂ assimilation and development responses were responsible for the response of biomass accumulation in tissues. However, the diversity of underlying physiological processes presented above would result in a wide diversity of carbon

assimilation per unit of plant development. Experimenters need to be aware of these factors, and this model should be built on or adjusted to account for them, to suit any particular experimental system.

Conclusion

Models based on data collected under controlled conditions were developed to predict net CO₂ assimilation rate per unit of plant development under various temperature scenarios. This unit for expressing biomass accumulation rate (i) summarized the effect of the temperature responses of development, respiration and photosynthesis, (ii) provided a means of comparing rates of biomass accumulation obtained under different growth conditions, independent of the effects of temperature on development, and (iii) represents a potential approach for quantifying irreversible versus reversible responses that may occur in the extremely high temperature range. The model is likely to require modification under certain circumstances, e.g., where acclimation, photosynthate mobilization processes, and genotypic variation are additional factors in temperature responses.

ACKNOWLEDGEMENTS

The authors thank Dr. Everard Edwards for precious advice on gas exchange measurements, and Dr. Pierre Martre and Dr. Denis Vile for useful comments on the manuscript.

SOURCES OF FUNDING

This work was supported by the European projects FP7-244374 (DROPS) and FP7-613817 (MODEXTREME) and the Grains Research and Development Corporation (GRDC) project UA00123. ACPFG was also funded by the GRDC, the Australian Research Council, the Government of South Australia and the University of Adelaide.

CONTRIBUTIONS BY AUTHORS

Iman Lohraseb carried out most experiments; Nicholas C. Collins contributed to interpretation of the data and preparation of the manuscript; Boris Parent performed most analyses and prepared the manuscript

SUPPORTING INFORMATION

The following [**SUPPORTING INFORMATION**] is available in the online version of this article:

Figure S1: Mass per leaf area in different leaves and thermal treatments

Figure S2: Simulation of the effect of night temperature on time courses of grain dry weight

Table S1: Summary of data coming from the literature.

Table S2: Phenotypic data measured in Experiment 2.

Method S1: Fitting procedures and parameters obtained for leaf senescence or growth of individual grain weight.

LITERATURE CITED

- Alkhatib K, Paulsen GM. 1984. Mode of high-temperature injury to wheat during grain development. *Physiologia Plantarum*, 61: 363-368.
- Atkin OK, Scheurwater I, Pons TL. 2006. High thermal acclimation potential of both photosynthesis and respiration in two lowland *Plantago* species in contrast to an alpine congeneric. *Global Change Biology*, 12: 500-515.
- Atkin OK, Scheurwater I, Pons TL. 2007. Respiration as a percentage of daily photosynthesis in whole plants is homeostatic at moderate, but not high, growth temperatures. *New Phytologist*, 174: 367-380.
- Atkin OK, Tjoelker MG. 2003. Thermal acclimation and the dynamic response of plant respiration to temperature. *Trends in Plant Science*, 8: 343-351.
- Barnabas B, Jager K, Feher A. 2008. The effect of drought and heat stress on reproductive processes in cereals. *Plant, Cell & Environment*, 31: 11-38.
- Ben-Haj-Salah H, Tardieu F. 1995. Temperature affects expansion rate of maize leaves without change in spatial distribution of cell length: Analysis of the coordination between cell division and cell expansion. *Plant Physiology*, 109: 870.
- Ben-Haj-Salah H, Tardieu F. 1997. Control of leaf expansion rate of droughted maize plants under fluctuating evaporative demand - A superposition of hydraulic and chemical messages? *Plant Physiology*, 114: 893-900.

- Berry J, Bjorkman O. 1980. Photosynthetic response and adaptation to temperature in higher-plants. *Annual Review of Plant Physiology and Plant Molecular Biology*, 31: 491-543.
- Borras-Gelonch G, Slafer GA, Casas AM, van Eeuwijk F, Romagosa I. 2010. Genetic control of pre-heading phases and other traits related to development in a double-haploid barley (*Hordeum vulgare* L.) population. *Field Crops Research*, 119: 36-47.
- Campbell C, Atkinson L, Zaragoza-Castells J, Lundmark M, Atkin O, Hurry V. 2007. Acclimation of photosynthesis and respiration is asynchronous in response to changes in temperature regardless of plant functional group. *New Phytologist*, 176: 375-389.
- O'Connell MG, O'Leary GJ, Whitfield DM, Connor DJ. 2004. Interception of photosynthetically active radiation and radiation-use efficiency of wheat, field pea and mustard in a semi-arid environment. *Field Crops Research*, 85: 111-124.
- Dell AI, Pawar S, Savage VM. 2011. Systematic variation in the temperature dependence of physiological and ecological traits. *Proceedings of the National Academy of Sciences of the United States of America*, 108: 10591-10596.
- Fang S, Cammarano D, Zhou G, Tan K, Ren S. 2015. Effects of increased day and night temperature with supplemental infrared heating on winter wheat growth in North China. *European Journal of Agronomy*, 64: 67-77.
- Gillooly JF, Brown JH, West GB, Savage VM, Charnov EL. 2001. Effects of size and temperature on metabolic rate. *Science*, 293: 2248 - 2251.

- Glaubitz U, Li X, Koehl KI, van Dongen JT, Hinch DK, Zuther E. 2014. Differential physiological responses of different rice (*Oryza sativa*) cultivars to elevated night temperature during vegetative growth. *Functional Plant Biology*, 41: 437-448.
- Johnson FH, Eyring H, Williams RW. 1942. The nature of enzyme inhibitions in bacterial luminescence: Sulfanilamide, urethane, temperature and pressure. *Journal of Cellular and Comparative Physiology*, 20: 247-268.
- Kanno K, Makino A. 2010. Increased grain yield and biomass allocation in rice under cool night temperature. *Soil Science and Plant Nutrition*, 56: 412-417.
- Kruse J, Rennenberg H, Adams MA. 2011. Steps towards a mechanistic understanding of respiratory temperature responses. *New Phytologist*, 189: 659-677.
- Kumudini S, Andrade FH, Boote KJ, Brown GA, Dzotsi KA, Edmeades GO, Gocken T, Goodwin M, Halter AL, Hammer GL, Hatfield JL, Jones JW, Kemanian AR, Kim SH, Kiniry J, Lizaso JI, Nendel C, Nielsen RL, Parent B, Stoeckle CO, Tardieu F, Thomison PR, Timlin DJ, Vyn TJ, Wallach D, Yang HS, Tollenaar M. 2014. Predicting Maize Phenology: Intercomparison of Functions for Developmental Response to Temperature. *Agronomy Journal*, 106: 2087-2097.
- Louarn G, Andrieu B, Giauffret C. 2010. A size-mediated effect can compensate for transient chilling stress affecting maize (*Zea mays*) leaf extension. *New Phytologist*, 187: 106-118.

- Loveys BR, Scheurwater I, Pons TL, Fitter AH, Atkin OK. 2002. Growth temperature influences the underlying components of relative growth rate: an investigation using inherently fast- and slow-growing plant species. *Plant Cell and Environment*, 25: 975-987.
- Makowski D, Asseng S, Ewert F, Bassu S, Durand JL, Li T, Martre P, Adam M, Aggarwal PK, Angulo C, Baron C, Basso B, Bertuzzi P, Biernath C, Boogaard H, Boote KJ, Bouman B, Bregaglio S, Brisson N, Buis S, Cammarano D, Challinor AJ, Confalonieri R, Conijn JG, Corbeels M, Deryng D, De Sanctis G, Doltra J, Fumoto T, Gaydon D, Gayler S, Goldberg R, Grant RF, Grassini P, Hatfield JL, Hasegawa T, Heng L, Hoek S, Hooker J, Hunt LA, Ingwersen J, Izaurrealde RC, Jongschaap REE, Jones JW, Kemanian RA, Kersebaum KC, Kim SH, Lizaso J, Marcaida M, III, Mueller C, Nakagawa H, Kumar SN, Nendel C, O'Leary GJ, Olesen JE, Oriol P, Osborne TM, Palosuo T, Pravia MV, Priesack E, Ripoche D, Rosenzweig C, Ruane AC, Ruget F, Sau F, Semenov MA, Shcherbak I, Singh B, Singh U, Soo HK, Steduto P, Stoeckle C, Stratonovitch P, Streck T, Supit I, Tang L, Tao F, Teixeira EI, Thorburn P, Timlin D, Travasso M, Roetter RP, Waha K, Wallach D, White JW, Wilkens P, Williams JR, Wolf J, Yin X, Yoshida H, Zhang Z, Zhu Y. 2015. A statistical analysis of three ensembles of crop model responses to temperature and CO₂ concentration. *Agricultural and Forest Meteorology*, 214: 483-493.
- Morita S, Yonemaru J, Takanashi J. 2005. Grain growth and endosperm cell size under high night temperatures in rice (*Oryza sativa* L.). *Annals of Botany*, 95: 695-701.

- Parent B, Conejero G, Tardieu F. 2009. Spatial and temporal analysis of non-steady elongation of rice leaves. *Plant Cell and Environment*, 32: 1561-1572.
- Parent B, Suard B, Serraj R, Tardieu F. 2010a. Rice leaf growth and water potential are resilient to evaporative demand and soil water deficit once the effects of root system are neutralized. *Plant Cell and Environment*, 33: 1256-1267.
- Parent B, Tardieu F. 2012. Temperature responses of developmental processes have not been affected by breeding in different ecological areas for 17 crop species. *The New phytologist*, 194: 760-74.
- Parent B, Tardieu F. 2014. Can current crop models be used in the phenotyping era for predicting the genetic variability of yield of plants subjected to drought or high temperature? *Journal of Experimental Botany*, 65: 6179-6189.
- Parent B, Turc O, Gibon Y, Stitt M, Tardieu F. 2010b. Modelling temperature-compensated physiological rates, based on the co-ordination of responses to temperature of developmental processes. *Journal of Experimental Botany*, 61: 2057-2069.
- Peng SB, Huang JL, Sheehy JE, Laza RC, Visperas RM, Zhong XH, Centeno GS, Khush GS, Cassman KG. 2004. Rice yields decline with higher night temperature from global warming. *Proceedings of the National Academy of Sciences of the United States of America*, 101: 9971-9975.
- Peraudeau S, Rogues S, Quinones CO, Fabre D, Van Rie J, Ouwkerk PBF, Jagadish KSV, Dingkuhn M, Lafarge T. 2015. Increase in night

temperature in rice enhances respiration rate without significant impact on biomass accumulation. *Field Crops Research*, 171: 67-78.

Poire R, Wiese-Klinkenberg A, Parent B, Mielewczik M, Schurr U, Tardieu F, Walter A. 2010. Diel time-courses of leaf growth in monocot and dicot species: endogenous rhythms and temperature effects. *Journal of Experimental Botany*, 61: 1751-1759.

Poorter H, Niinemets U, Poorter L, Wright IJ, Villar R. 2009. Causes and consequences of variation in leaf mass per area (LMA): a meta-analysis. *New Phytologist*, 182: 565-588.

Poorter H, Niklas KJ, Reich PB, Oleksyn J, Poot P, Mommer L. 2012. Biomass allocation to leaves, stems and roots: meta-analyses of interspecific variation and environmental control. *New Phytologist*, 193: 30-50.

Porter JR. 2005. Rising temperatures are likely to reduce crop yields. *Nature*, 436: 174-174.

Reynolds M, Bonnett D, Chapman SC, Furbank RT, Manes Y, Mather DE, Parry MAJ. 2011. Raising yield potential of wheat. I. Overview of a consortium approach and breeding strategies. *Journal of Experimental Botany*, 62: 439-452.

Reynolds M, Foulkes MJ, Slafer GA, Berry P, Parry MAJ, Snape JW, Angus WJ. 2009. Raising yield potential in wheat. *Journal of Experimental Botany*, 60: 1899-1918.

Rosenzweig C, Jones JW, Hatfield JL, Ruane AC, Boote KJ, Thorburn P, Antle JM, Nelson GC, Porter C, Janssen S, Asseng S, Basso B, Ewert F, Wallach D, Baigorria G, Winter JM. 2013. The Agricultural Model

- Intercomparison and Improvement Project (AgMIP): Protocols and pilot studies. *Agricultural and Forest Meteorology*, 170: 166-182.
- Sadok W, Naudin P, Boussuge B, Muller B, Welcker C, Tardieu F. 2007. Leaf growth rate per unit thermal time follows QTL-dependent daily patterns in hundreds of maize lines under naturally fluctuating conditions. *Plant Cell and Environment*, 30: 135 - 146.
- Sage RF, Kubien DS. 2007. The temperature response of C-3 and C-4 photosynthesis. *Plant Cell and Environment*, 30: 1086-1106.
- Slafer GA, Rawson HM. 1994. Sensitivity of wheat phasic development to major environmental factors. A reexamination of some assumptions made by physiologists and modellers. *Australian Journal of Plant Physiology*, 21: 393-426.
- Tardieu F, Granier C, Muller B. 1999. Modelling leaf expansion in a fluctuating environment: are changes in specific leaf area a consequence of changes in expansion rate? *New Phytologist*, 143: 33-44.
- Tashiro T, Wardlaw IF. 1990. The effects of high temperature at different stages of ripening on grain set, grain weight and grain dimensions in the semi dwarf wheat "Banks". *Annals of Botany*, 65: 51-61.
- Taub DR, Seemann JR, Coleman JS. 2000. Growth in elevated CO₂ protects photosynthesis against high-temperature damage. *Plant Cell and Environment*, 23: 649-656.
- Vasseur F, Pantin F, Vile D. 2011. Changes in light intensity reveal a major role for carbon balance in Arabidopsis responses to high temperature. *Plant Cell and Environment*, 34: 1563-1576.

- Vile D, Pervent M, Belluau M, Vasseur F, Bresson J, Muller B, Granier C, Simonneau T. 2012. Arabidopsis growth under prolonged high temperature and water deficit: independent or interactive effects? *Plant Cell and Environment*, 35: 702-718.
- Wardlaw IF. 1994. The effect of high temperature on kernel development in wheat: Variability related to pre-heading and postanthesis conditions. *Australian Journal of Plant Physiology*, 21: 731-739.
- Wardlaw IF, Blumenthal C, Larroque O, Wrigley CW. 2002. Contrasting effects of chronic heat stress and heat shock on kernel weight and flour quality in wheat. *Functional Plant Biology*, 29: 25-34.
- Wardlaw IF, Dawson IA, Munibi P. 1989a. The tolerance of wheat to high temperatures during reproductive growth. 2. Grain development. *Australian Journal of Agricultural Research*, 40: 15-24.
- Wardlaw IF, Dawson IA, Munibi P, Fewster R. 1989b. The tolerance of wheat to high temperatures during reproductive growth. 1. Survey procedures and general response patterns *Australian Journal of Agricultural Research*, 40: 1-13.
- Wardlaw IF, Moncur L. 1995. The response of wheat to high-temperature following anthesis. 1. The rate and duration of kernel filling. *Australian Journal of Plant Physiology*, 22: 391-397.
- Warrington IJ, Kanemasu ET. 1983. Corn growth response to temperature and photoperiod. 1. Seedling emergence, tassel initiation, and anthesis. *Agronomy Journal*, 75: 749-754.
- Welch JR, Vincent JR, Auffhammer M, Moya PF, Dobermann A, Dawe D. 2010. Rice yields in tropical/subtropical Asia exhibit large but opposing

sensitivities to minimum and maximum temperatures. *Proceedings of the National Academy of Sciences of the United States of America*, 107: 14562-14567.

Wheeler TR, Hong TD, Ellis RH, Batts GR, Morison JIL, Hadley P. 1996. The duration and rate of grain growth, and harvest index, of wheat (*Triticum aestivum* L) in response to temperature and CO₂. *Journal of Experimental Botany*, 47: 623-630.

Yin X, Guo W, Spiertz JH. 2009. A quantitative approach to characterize sink-source relationships during grain filling in contrasting wheat genotypes. *Field Crops Research*, 114: 119-126.

Zahedi M, Sharma R, Jenner CF. 2003. Effects of high temperature on grain growth and on the metabolites and enzymes in the starch-synthesis pathway in the grains of two wheat cultivars differing in their responses to temperature. *Functional Plant Biology*, 30: 291-300.

Zhao H, Dai T, Jing Q, Jiang D, Cao W. 2007. Leaf senescence and grain filling affected by post-anthesis high temperatures in two different wheat cultivars. *Plant Growth Regulation*, 51: 149-158.

FIGURE LEGENDS

Figure 1. Temperature responses (experiment 1) of leaf elongation rate (LER), daily net photosynthesis (P_N), daily dark respiration (R) and daily net CO_2 assimilation per day (A_N) expressed with time (d) or developmental time units ($A_{N,20^\circ C}$, $d_{20^\circ C}$). Dots: average values; error bars: confidence intervals ($p = 0.95$); lines: regression from Eq.2. **a)** LER ($n > 8$). **b)** P_N (squares), R (triangles) and A_N (circles) ($n > 4$). **c)** LER (black dots) and A_N (white dots) normalised by their respective values at $20^\circ C$. Dashed line displays the temperature response of A_N under saturating light. **d)** $A_{N,20^\circ C}$.

Figure 2. Leaf elongation rate (LER, **a**), net CO_2 assimilation per day (A_N , **b**) or day at $20^\circ C$ ($A_{N,20^\circ C}$, **c**), leaf dry mass per area (LMA, averaged for leaves 4, 5, 6 and 7, **d**) and the relationship between $A_{N,20^\circ C}$ and LMA (**e**) under four different temperature scenarios ($T^\circ_{day} / T^\circ_{night}$, experiment 2). Bars: average values ($n = 6$); error bars: confidence intervals ($p = 0.95$). Means with the same letter indicate that there were no significant differences in a pairwise t-test.

Figure 3. Time courses of leaf chlorophyll amount (SPAD units) under different temperature regimes (experiment 3), $20/15^\circ C$ (blue), $20/20^\circ C$ (green), $25/15^\circ C$ (red) and $25/20^\circ C$ (orange). Time is expressed either as day (d, **a**) or developmental time ($d_{20^\circ C}$, **b**). Dots: average values ($n \geq 4$). Error bar: average confidence intervals ($p = 0.95$). Lines are bilinear regressions with 3 parameters ($SPAD_0$, t_s , a_s). $SPAD_0$ is fixed and common to all treatments. **Inset in a)** Values of t_s . Bars: parameter value \pm confidence interval calculated by bootstrap ($p = 0.95$). **Inset in b)** Values of $t_{s,20^\circ C}$. Bars: parameter value \pm confidence interval ($p = 0.95$).

Figure 4. Time courses of individual grain dry weight (GDW) under different temperature regimes (experiment 3), 20/15°C (blue), 20/20°C (green), 25/15°C (red), 25/20°C (orange). Time is expressed either as days (**a,c**) or developmental time ($d_{20^{\circ}\text{C}}$, **b**). M : grain maturity. Dots: average values ($n \geq 4$). Error bars: average confidence intervals ($p = 0.95$). Lines are logistic regressions with 3 parameters (W_0 , t_0 , λ). W_0 is fixed and common to all treatments. **a**) λ and t_0 are free in each treatment. **Inset in a**) values of $t_0 \pm$ confidence interval ($p = 0.95$). **b**) λ and t_0 are free in each treatment but with time expressed as developmental time ($d_{20^{\circ}\text{C}}$). **Inset in b**) values of $t_{0,20^{\circ}\text{C}} \pm$ confidence interval ($p = 0.95$). **c**) λ is the only free parameter in each treatment. t_0 (d) is calculated in each treatment from a single $t_{0,20^{\circ}\text{C}}$ value ($d_{20^{\circ}\text{C}}$), common to all treatments.

Figure 5. Values of maximum grain growth rate (GGR_{max} , **a**) estimated from regression displayed in Fig.4c (W_0 and t_0 fixed), expressed with time (black bars) or developmental time units (white bars), and the relationship between net CO_2 assimilation per $d_{20^{\circ}\text{C}}$ ($A_{N,20^{\circ}\text{C}}$) and final individual grain weight or $\text{GGR}_{\text{max},20^{\circ}\text{C}}$ in the 4 different temperature scenarios (**b**). **a**) Bars: estimated parameter value. Error bar: confidence interval ($p = 0.95$). **b**) Grey triangles: final grain weight. White circles: $\text{GGR}_{\text{max},20^{\circ}\text{C}}$. $A_{N,20^{\circ}\text{C}}$ values were measured in Experiment 2 and shown in Fig 2 and SUPPORTING INFORMATION Table S2.

Figure 6. Observed values vs. calculated values for the reduction in final grain weight between temperatures treatments. Observed data come from the literature (see SUPPORTING INFORMATION Table S1). Dashed line is the model $x=y$.

Figure 1

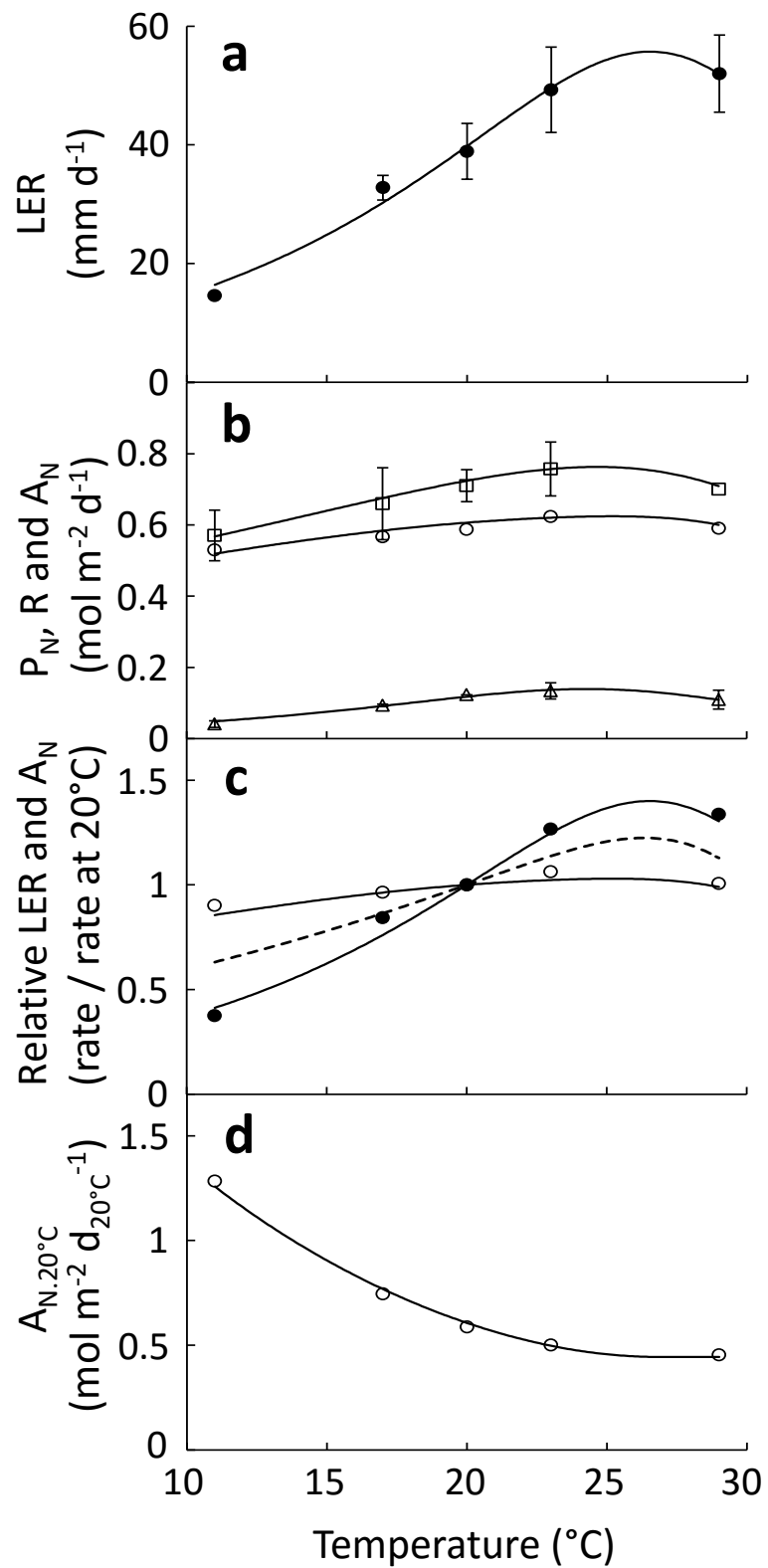


Figure 2

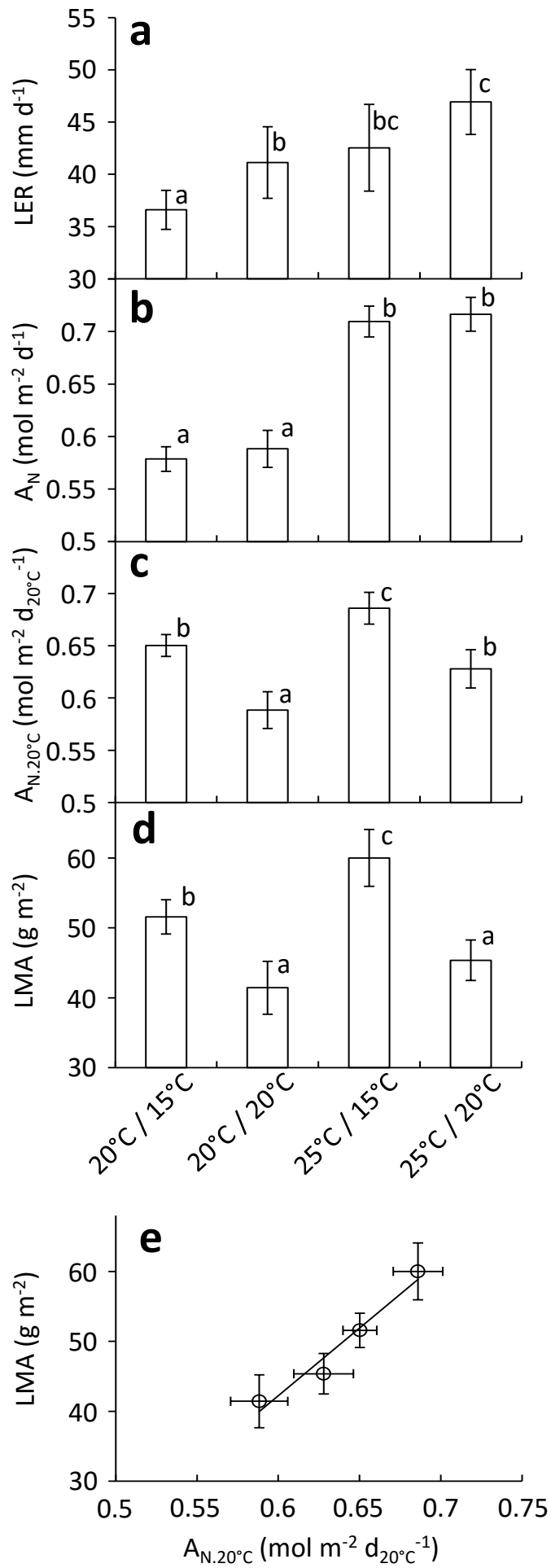


Figure 3

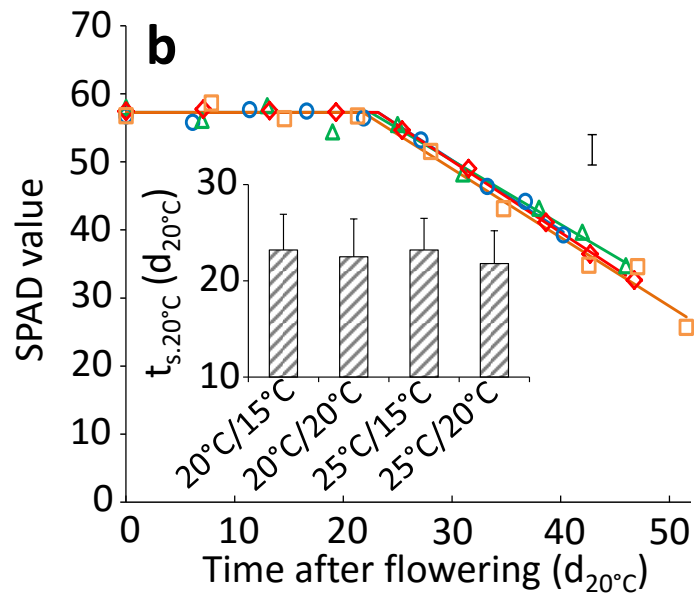
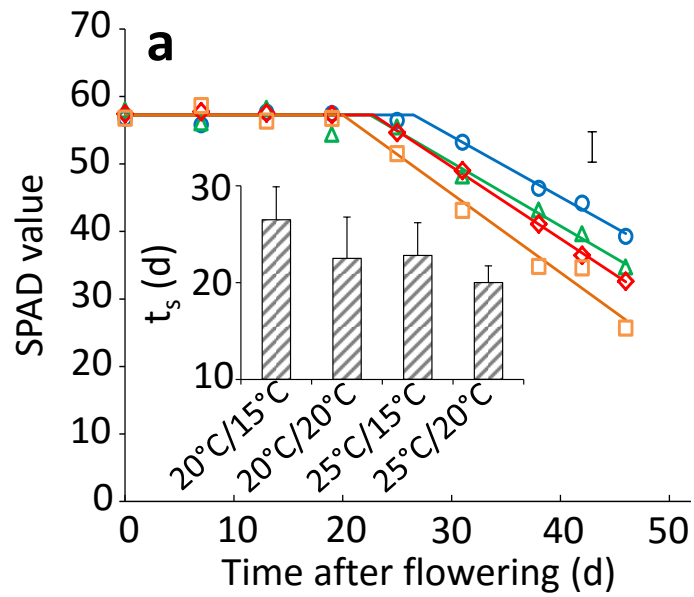


Figure 4

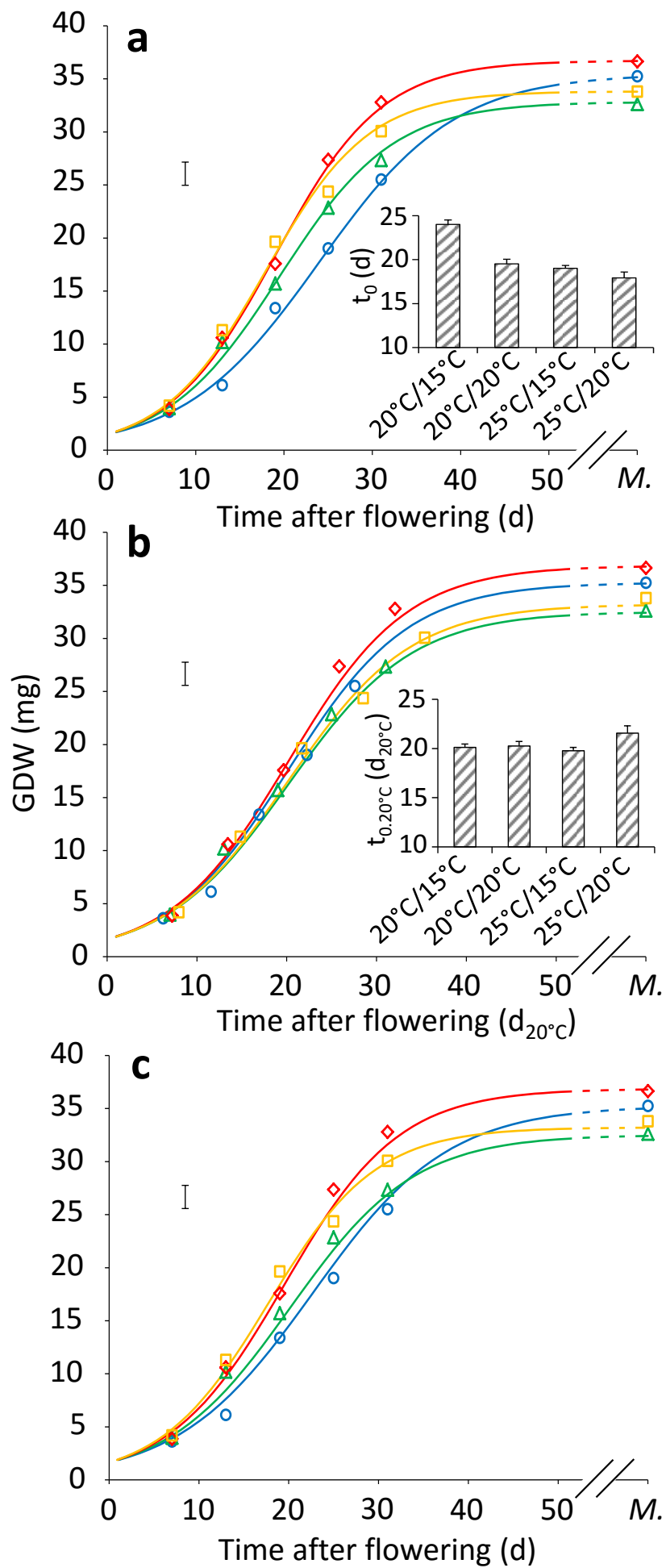


Figure 5

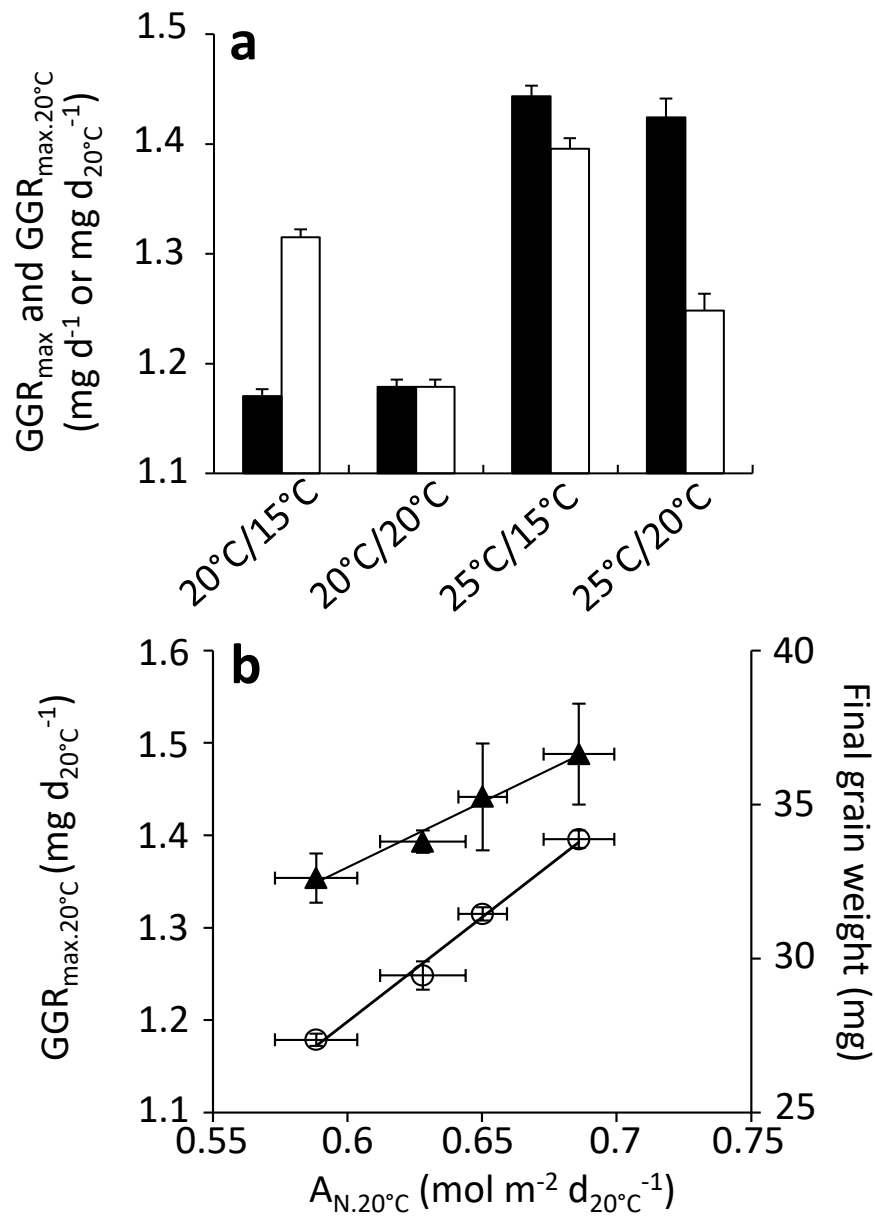


Figure 6

